

Research Article

CFD-DEM Simulation of Reverse Circulation Pneumatic Cuttings Removal during Coal Seam Drilling

Xiaoming Han , Peibo Li, and Jialiang Li

School of Mechanical and Power Engineering, Henan Polytechnic University, Henan, Jiaozuo 454003, China

Correspondence should be addressed to Xiaoming Han; hanxmr@126.com

Received 10 June 2020; Revised 31 July 2020; Accepted 14 August 2020; Published 30 September 2020

Academic Editor: Ahmad Zeeshan

Copyright © 2020 Xiaoming Han et al. This is an open access article distributed under the Creative Commons Attribution License, which permits unrestricted use, distribution, and reproduction in any medium, provided the original work is properly cited.

To solve the problems that the borehole depth is shallow and the borehole formation rate is low during the gas drainage drilling in soft coal seam with current cuttings removal method, a new technology of reverse circulation pneumatic cuttings removal is put forward. The CFD-DEM coupling method is used to establish the simulation model of cuttings-air two-phase flow in drill pipe. The effects of the air velocity for cuttings removal and the mass flow rate of cuttings on the flow characteristics, cuttings removal effect and pressure drop of cuttings-gas two-phase flow are analysed. The results show that the drag force of drilling cuttings becomes larger with the increase of air velocity and the stratified flow characteristic is obvious. The drill cuttings migration ratio is positively correlated with the air velocity for cuttings removal and negatively correlated with the mass flow rate of cuttings. When the mass flow rate of cuttings is constant, the increase of air velocity for cuttings removal leads to the increase of pressure drop in the inner hole of drill pipe. When the air velocity of cuttings removal is constant, the mass flow rate of cuttings and the pressure drop in the inner hole of drill pipe increases. Therefore, the appropriate air velocity should be selected considering the energy consumption during cuttings removal.

1. Introduction

Gas extraction is the main means to prevent and control gas outburst in coal seam. And, drill cuttings conveying during the borehole drilling in coal seam is the key to ensure the drilling depth and the drilling efficiency. The mechanical removal and the hydraulic removal of cuttings have a great impact on the stability of borehole wall, which is easy to cause the borehole collapse and blockage, sticking of the drill pipe, and other accidents [1]. The current cuttings removal method with pressure air removes the cuttings through the annular hole between drill pipe and borehole wall by the pressure air through the inner hole of drill pipe. It is difficult to collect the drill cuttings at the outlet of boreholes, which is easy to cause the dust pollution [2–4]. So, a new reverse circulation pneumatic cuttings removal technology is proposed that the annular hole between drill pipe and borehole wall is used as the air inlet and the inner hole of drill pipe is used as the cuttings removal channel [5, 6].

Numerical methods based on computational fluid dynamics (CFD) have mainly been used. Niu and Zhang [7] studied the critical wind speed under different cuttings removal rate and solid gas ratio as well as the pressure loss of air flow in drill pipe inner hole and annular hole. It is found that the critical wind speed and pressure loss are positively correlated with the solid gas ratio. Guo et al. [8] performed three dimensional and time-dependent calculations by using the finite volume CFD of sudden pipe expansion flows. Riaz and Sadiq [9] set up the governing equations with the help of similarity transformations and handled the solution of boundary value problems by perturbation procedure. So, the analytical solutions for fluid and particulate phase velocities, mean flow rates, and pressure gradient profile have been presented, while a numerical treatment has been carried out for pressure rise. And, the exact solutions of non-Newtonian multiphase fluid through peristaltic pumping characteristics in an annulus having compliant walls and applied magnetic field was studied [10]. Abdelsalam et al. [11] and Ijaz et al.

[12] studied the two-phase flows characteristics in the biologically inspired pumping systems.

The Computational Fluid Dynamics and Discrete Element Method Coupling Algorithm (CFD-DEM) is a well-developed method that has been proven effective in the study of liquid-solid and gas-solid two-phase flow system. The bilateral coupled CFD-DEM method was used to numerically simulate the coal particles flow pattern in the swirling pneumatic conveying process and the interaction between coal particles and pipe wall to reveal the mechanism of coal particle swirling pneumatic conveying [13, 14]. Based on the CFD-DEM coupling algorithm, the dust cyclone separator in negative pressure fixed-point sampling is simulated to study the effect of air velocity and coal mass flow rate on the coal-air two-phase separation process [15]. Akhshik et al. [16, 17] applied the CFD-DEM coupling method to study the effects of drill pipe rotation and drill cuttings shape on the cuttings flow characteristics in different inclined angle drilling holes. And, the numerical simulation is consistent with the experimental results. Based on the CFD-DEM coupling method, Shao et al. [18] simulated the migration of large-diameter unconventional drill cuttings particles to study the drill cuttings removal rule in borehole and reveal the influence of cuttings shape and content on the removal effect of cuttings. Sun et al. [19] used the CFD-DEM coupling method to simulate the trajectory of drill cuttings. The simulation results of the cuttings concentration coincided with the experimental data by Kim et al. [20], which proved the accuracy and feasibility of the CFD-DEM coupling method in the drill cuttings removal. Therefore, the CFD-DEM coupling method is also used to simulate the cuttings-gas two-phase flow in the inner hole of drill pipe during the horizontal drilling borehole in coal seam. The research can reveal the effects of the air velocity for cuttings removal and the mass flow rate of cuttings on the flow characteristics, cuttings removal effect, and pressure drop of cuttings-gas two-phase flow to improve the drilling efficiency in coal seam.

2. Materials and Methods

2.1. Introduction of the Reverse Circulation Pneumatic Cuttings Removal System. As shown in Figure 1, the reverse circulation pneumatic cuttings removal system mainly includes drilling rig, drill pipe, drilling bit, cyclone separator, and Roots vacuum pump. The Roots vacuum pump provides the air force for the pneumatic conveying of drill cuttings. Under the suction effect of vacuum pump, air enters the bottom of the drill hole along the annular hole between drill pipe and borehole wall. The drill cuttings generated by the operating drilling bit are wrapped and carried into the inner hole of drill pipe through the discharge hole. And, the inner hole of drill pipe is used as the cuttings removal channel. The cyclone separator acts as the dust removal device to separate the drill cuttings from the cuttings-air two-phase flow. The drill cuttings are collected in the separator under the gravity while the filtered air is discharged through the Roots vacuum pump. The system has high removal efficiency of drill cuttings and plays a role of dust control and dust suppression by collecting the discharged cuttings.

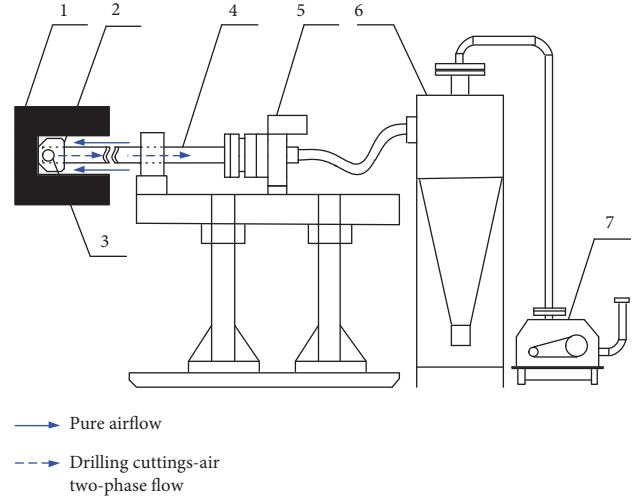


FIGURE 1: System composition of reverse circulation pneumatic cuttings removal. 1-Coal wall; 2-Drilling bit; 3-Discharge hole; 4-Drill pipe; 5-Drilling rig; 6-Cyclone separator; 7-Roots vacuum pump.

2.2. Drill Cuttings-Air Two-Phase Flow Control Equation. The drill cuttings generated by the drilling bit breaking coal are smaller in size. Considering the continuity and fluidity of a large number of drill cuttings along the inner hole of drill pipe are similar to the movement of fluid, the dual-Eulerian model is used to describe the two-phase flow of drill cuttings and air. The air phase control equation includes the mass conservation and momentum conservation equations [16, 17, 21]:

$$\begin{aligned} \frac{\partial(\epsilon_a \rho_a)}{\partial t} + \nabla \cdot (\epsilon_a \rho_a \mathbf{v}_a) &= 0, \\ \frac{\partial(\epsilon_a \rho_a \mathbf{v}_a)}{\partial t} + \nabla \cdot (\epsilon_a \rho_a \eta \mathbf{v}_a) &= -\nabla p + \nabla \cdot (\epsilon_a \eta \nabla \mathbf{v}_a) + \epsilon_a \rho_a \mathbf{g} - \mathbf{S}, \end{aligned} \quad (1)$$

where, ϵ_a is the porosity, ρ_a is the air density, \mathbf{v}_a is the air velocity, ∇ is the divergence operator, p is the pressure on a fluid mesh element, η is the aerodynamic viscosity, and \mathbf{S} is the momentum sink which is the ratio of the sum of the forces between drill cuttings and air in the fluid mesh unit to the volume of the fluid mesh unit:

$$\mathbf{S} = \frac{\sum_{i=1}^N \mathbf{F}_{c-a,i}}{V_{\text{cell}}}, \quad (2)$$

where N is the number of drill cuttings in the fluid mesh unit, $\mathbf{F}_{c-a,i}$ is the interaction force between drill cuttings and air, and V_{cell} is the fluid grid element volume.

$$\mathbf{F}_{c-a} = C_D \frac{\pi d_c^2}{8} (\mathbf{v}_a - \mathbf{v}_c)^2, \quad (3)$$

where C_D is the resistance coefficient, d_c is the drill cuttings diameter, and \mathbf{v}_c is the drilling speed.

The drill cuttings motion follows Newton's second law. So,

$$m_i \frac{d\mathbf{v}_i}{dt} = m_i \mathbf{g} + \mathbf{F}_{c-a,i} + \mathbf{F}_c, \quad (4)$$

$$\mathbf{I}_i \frac{d\boldsymbol{\omega}_i}{dt} = \sum_{j=1}^k \mathbf{T}_{ij} + \mathbf{T}_{DT,i},$$

where m_i is the quality of drill cuttings, \mathbf{v}_i is the drilling speed, \mathbf{F}_c is the contact force of drill cuttings, \mathbf{I}_i is the rotary inertia of drill cuttings, $\boldsymbol{\omega}_i$ is the angular velocity of drill cuttings, and $\sum_{j=1}^k \mathbf{T}_{ij}$ is the resultant moment of drill cuttings:

$$\mathbf{T}_{ij} = \mathbf{F}_c \times \mathbf{r}_i, \quad (5)$$

where, \mathbf{r}_i is the vector from the center of mass of cutting i to the contact point and $\mathbf{T}_{DT,i}$ is the moment produced by the slip-rotation:

$$\mathbf{T}_{DT,i} = \frac{\rho}{2} \left(\frac{d_i}{2} \right)^5 C_{DR} |\Omega| \Omega, \quad (6)$$

where ρ is the cutting density, d_i is the mean diameter of i th cutting, C_{DR} is the rotational drag coefficient, and Ω is the relative angular velocity of the cutting to the air.

2.3. Drill Cuttings Contact Model. During the movement of drill cuttings along the inner hole of drill pipe, the Hertz–Mindlin contact model is used to describe the cuttings-cuttings contact and the contact between the cuttings and the inner wall of drill pipe. The contact forces of drill cuttings are shown in Figure 2. The contact forces between the cuttings or between the cuttings and the inner wall of drill pipe are divided into normal force \mathbf{F}_n^c , normal damping force \mathbf{F}_n^d , tangential force \mathbf{F}_t^c , and tangential damping force \mathbf{F}_t^d .

The normal force \mathbf{F}_n^c is the function of normal overlap δ_n , equivalent Young's modulus Y^* , and equivalent radius R^* [13]:

$$\mathbf{F}_n^c = \frac{4}{3} Y^* \delta_n^{3/2} \sqrt{R^*}, \quad (7)$$

$$\frac{1}{Y^*} = \frac{(1 - \nu_i^2)}{Y_i} + \frac{(1 - \nu_j^2)}{Y_j}, \quad (8)$$

$$\frac{1}{R^*} = \frac{1}{R_i} + \frac{1}{R_j}, \quad (9)$$

where ν_i , Y_i , and R_i and ν_j , Y_j , and R_j are Poisson's ratio, Young's modulus, and radius of cuttings i and cuttings j , respectively.

The normal damping force \mathbf{F}_n^d is

$$\mathbf{F}_n^d = -2\sqrt{5/6}\gamma \sqrt{S_n m^*} \mathbf{v}_n^{rel}, \quad (10)$$

$$S_n = 2Y^* \sqrt{R^* \delta_n}, \quad (11)$$

$$\gamma = \frac{\ln e}{\sqrt{\ln^2 e + \pi^2}}, \quad (12)$$

$$\frac{1}{m^*} = \frac{1}{m_i} + \frac{1}{m_j}, \quad (13)$$

where S_n is the normal stiffness, m^* is the equivalent mass, \mathbf{v}_n^{rel} is the normal component of relative velocity between drill cuttings, e is the recovery coefficient, And m_i and m_j are the quality of drill cuttings i and drill cuttings j , respectively.

The tangential force \mathbf{F}_t^c depends on the tangential overlap δ_t and the tangential stiffness S_t :

$$\mathbf{F}_t^c = -S_t \delta_t, \quad (14)$$

$$S_t = 8G^* \sqrt{R^* \delta_t}, \quad (15)$$

$$G^* = \frac{2 - \nu_i^2}{G_i} + \frac{2 - \nu_j^2}{G_j}, \quad (16)$$

where G^* is the equivalent shear modulus and G_i and G_j are the shear modulus of cuttings i and cuttings j , respectively.

The tangential damping force \mathbf{F}_t^d is

$$\mathbf{F}_t^d = -2\sqrt{5/6}\gamma \sqrt{S_t m^*} \mathbf{v}_t^{rel}, \quad (17)$$

where \mathbf{v}_t^{rel} is the normal component of relative velocity between drill cuttings.

When the tangential force between the drill cuttings is greater than the static friction force, the slip between the drill cuttings will occur. The tangential force is

$$\mathbf{F}_t^c = \varphi_s \mathbf{F}_n^c, \quad (18)$$

where φ_s is the sliding friction coefficient.

2.4. Simulation Model. According to the working principle of the reverse circulation pneumatic cuttings removal system, the geometric model including borehole, drilling bit, and drill pipe is built, as shown in Figure 3.

According to the working principle of the reverse circulation pneumatic cuttings removal system, the diameter of drilling bit is 94 mm and the diameter of discharge hole in drilling bit is 40 mm. The outer diameter of drill pipe is 73 mm, and the inner hole diameter of drill pipe is 40 mm. The drilling bit is connected with the drill pipe. The diameter of the borehole in coal seam is about 100 mm. In order to analyze the flow characteristics of the drill cuttings along the inner hole of drill pipe, the length of drill pipe is set as 4.9 m and the drilling bit length is set as 0.1 m. So, the geometry model length of the drill pipe-bit reverse circulation pneumatic cuttings removal simulation is 5 m.

The hexahedral mesh is used to mesh the geometric model. A total of 53209 mesh elements and 47428 mesh nodes are generated. The mesh generation is shown in Figure 4. The annular hole between drill pipe and borehole wall is set as the inlet and the end of the inner hole of drill pipe is set as the outlet.

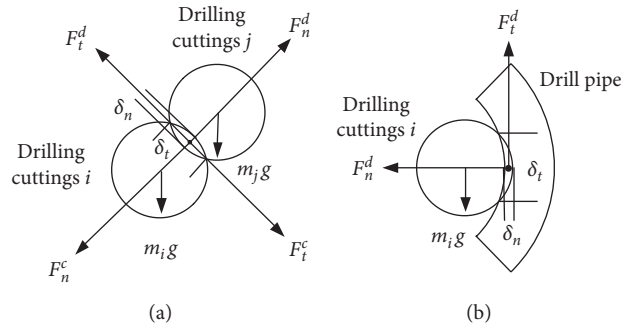


FIGURE 2: Scheme diagram of contact forces.



FIGURE 3: Geometric model.

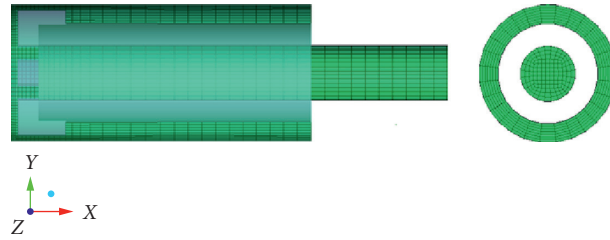


FIGURE 4: Mesh generation.

To solve the air phase, the unsteady pressure solver with a gravitational acceleration of 9.81 m/s^2 along the negative Y direction is set. The turbulence model is the realizable $k-\epsilon$ turbulence model. The inlet is set as speed inlet with the air velocity of 5.13 m/s, 6.85 m/s, 8.56 m/s, 10.27 m/s, and 11.98 m/s, respectively. Correspondingly, the air velocity in the inner hole of drill pipe is 15 m/s, 20 m/s, 25 m/s, 30 m/s, and 35 m/s, respectively. The turbulence intensity is 5%, and the turbulent viscosity ratio is 0.5. The outlet is set as pressure outlet with the pressure of -3000 Pa . The finite volume method and the QUICK algorithm are used to discretize the air phase control equation and the momentum equation. The second-order upwind scheme is used to discretize the turbulent kinetic energy and the turbulent diffusion equation. The SIMPLE algorithm is used for the phase-to-phase coupling of pressure-velocity phase. The simulation parameters are set as Table 1.

The drill cuttings generated by the drilling bit in coal seam were collected, and the particle size analysis was carried out. It was found that the particle size of the cuttings was mainly less than 1 mm. Therefore, the spherical particles with the particle

diameter of 1 mm were used to simulate the drill cuttings. The drill cuttings are generated at the entrance of the discharge hole of drilling bit. And, the cuttings production is set as 0.06 kg/s, 0.08 kg/s, 0.10 kg/s, 0.12 kg/s, and 0.14 kg/s, respectively. In order to avoid the drill cuttings accumulating at the discharge hole when the cuttings are generated, the initial velocity of cuttings is set as 2 m/s in the X direction. The drill cuttings phase solution time step is set to be $2 \times 10^{-6} \text{ s}$, and the air phase time step is set to be $1 \times 10^{-4} \text{ s}$.

2.5. Model Verification. To validate the simulation predictions, the reverse circulation pneumatic cuttings removal test device is built which is shown in Figure 5.

The Roots vacuum pump typed of QZSR125A is used as the power source of the experimental system. The boost range is $-50 \sim 0 \text{ kPa}$, and the maximum flow is $6.38 \text{ m}^3/\text{min}$. During the test, the flow of Roots vacuum pump can be changed by adjusting the speed of variable frequency motor of Roots vacuum pump to adjust the air velocity. A feeding device is used to simulate the generation of drill

TABLE 1: Settings of simulation parameters.

Item	Parameter	Unit	Value
Drill cuttings	Poisson ratio	—	0.3
	Shear modulus	Pa	1×10^9
	Density	kg/m ³	1400
Drill pipe	Poisson ratio	—	0.29
	Shear modulus	Pa	7.9×10^{10}
	Density	kg/m ³	7800
Contact of cuttings and cuttings	Contact model	—	Hertz-mindlin
	Recovery coefficient	—	0.5
	Static friction coefficient	—	0.6
	Rolling friction coefficient	—	0.05
Contact of drill cuttings and drill pipe inner wall	Contact model	—	Hertz-mindlin
	Recovery coefficient	—	0.5
	Static friction coefficient	—	0.4
	Rolling friction coefficient	—	0.05
Atmosphere	Density	kg/m ³	1.225
	Dynamic viscosity	kg/(m·s)	1.7894×10^{-5}

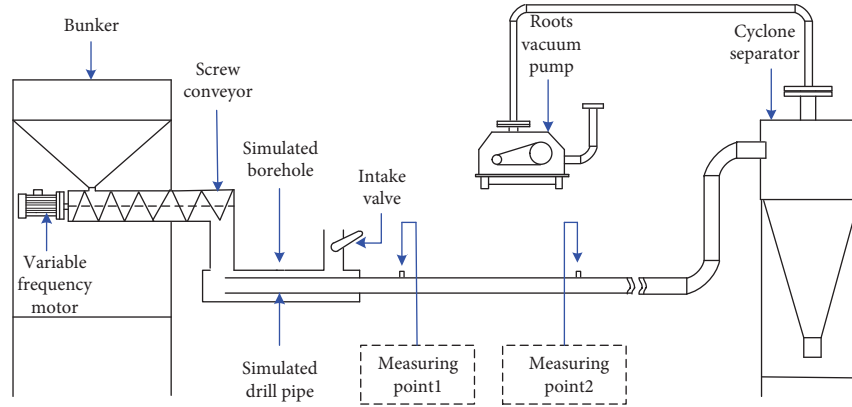


FIGURE 5: Experiment system of reverse circulation pneumatic cuttings removal.

cuttings. The feeding device is composed of bunker and screw conveyor. The mass flow rate of cuttings is controlled by adjusting the speed of screw conveyor. The transparent rigid plexiglass tube is used to simulate the drill pipe and borehole. The two-phase separation of drill cuttings and air is completed in the cyclone separator. In order to obtain the pressure drop of drill pipe under the steady flow of cuttings and air, the pressure measuring point 1 is set at the distance of 3 m from the drill pipe inlet, and the pressure measuring point 2 is set at the downstream 2 m from the pressure measuring point 1. Figure 6 is the actual experimental equipment.

In the experiment, the mass flow rate of cuttings was selected as 0.06 kg/s, 0.10 kg/s, and 0.14 kg/s, and the air velocity was selected as 15 m/s, 20 m/s, 25 m/s, 30 m/s, and 35 m/s. The pressure drop per unit length between measuring point 1 and measuring point 2 was tested and is shown in Figure 7. From the comparison of pressure drop per unit length, it shows that the results of CFD-DEM simulation reasonably agree with those of the experiment.

3. Results and Discussion

3.1. Flow Characteristics Analysis of Cuttings Phase

3.1.1. Drilling Cuttings Flow Pattern in Inner Hole of Drill Pipe. The cuttings flow patterns of 0~0.5 m and 4.5~5 m segments in the inner hole of drill pipe under different air velocities are shown in Figure 8 when the cuttings mass flow rate is 0.14 kg/s.

From Figure 8, it can be seen that the drilling cuttings are evenly generated at the entrance of the discharge hole of drilling bit. Then, the cuttings enter the inner hole of drill pipe at the initial speed of 2 m/s. Because the cuttings speed is less than the air velocity, the drilling cuttings accelerate and form obvious cuttings flow under the drag force of air flow, and then under the gravity action, the drilling cuttings flow gathers at the bottom of the inner hole of drill pipe and moves along the direction of the air flow until they are discharged from the inner hole of drill pipe.

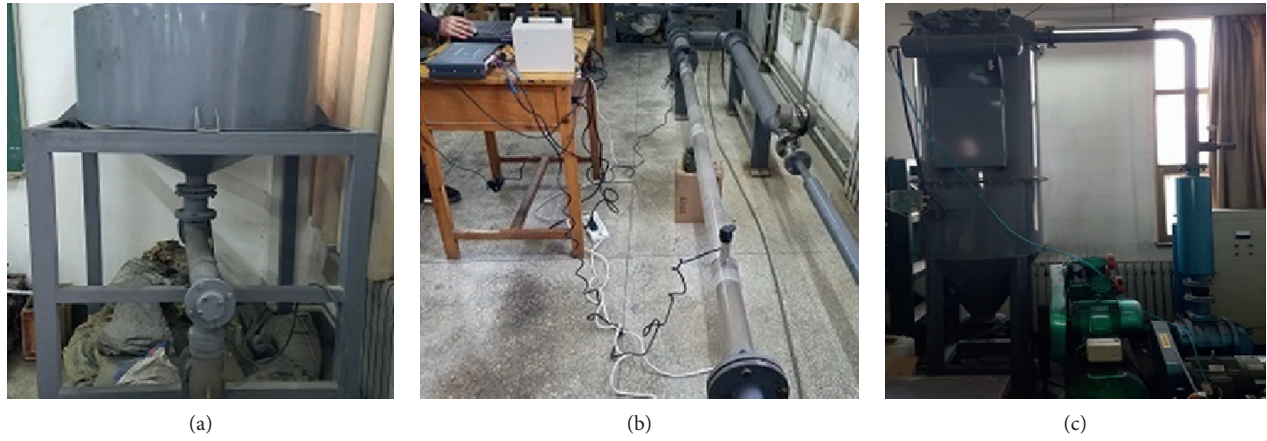


FIGURE 6: Experimental equipment: (a) feeding device, (b) cuttings removal channel, and (c) separator and vacuum pump.

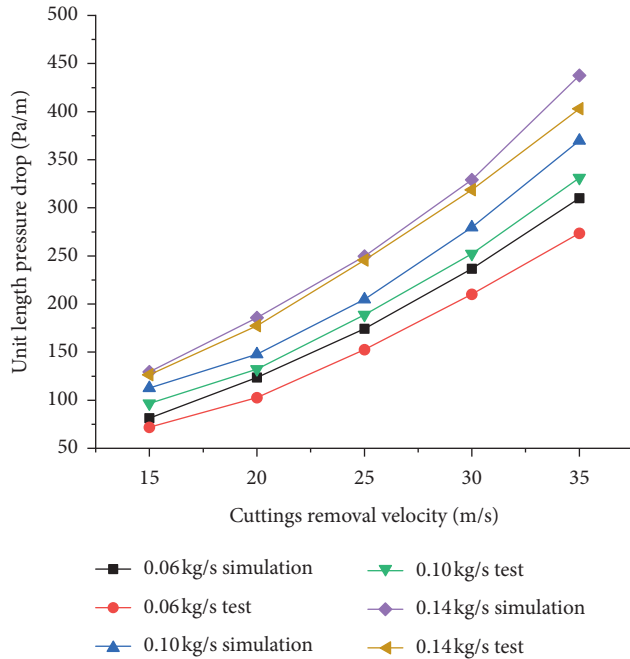


FIGURE 7: Comparison of pressure drop per unit length

When the air velocity is 15 m/s, the cuttings flow pattern is shown in Figure 8(a). Because of the low air velocity, the characteristic length of the cuttings flow is relatively short and deposits at the bottom of the inner hole of drill pipe. The typical characteristics of pipe bottom flow are presented along the flow direction and a thicker cuttings layer is formed. The moving speed of cuttings in the 4.5~5 m segment is obviously lower than that in the 0~0.5 m segment, which indicates that the cuttings have decelerated during the movement. When the air velocity is 20 m/s, the cuttings flow pattern is shown in Figure 8(b). With the increase of air velocity, the drag force of drilling cuttings becomes larger, and the characteristic length of drilling cuttings flow becomes longer. However, it still shows the characteristics of pipe bottom flow and the thickness of the drilling cuttings layer decreases. At this time, the moving speed of drilling

cuttings in the 4.5~5 m segment is higher than that in the 0~0.5 m segment. As shown in Figure 8(c), when the air velocity is 25 m/s, the characteristics of the cuttings flow are further lengthened, and the thickness of the cuttings layer decreases again along the flow direction. Individual drilling cuttings are distributed in the upper part of the inner hole of drill pipe. As shown in Figure 8(d), when the air velocity is 30 m/s, the characteristics length of the cuttings flow becomes longer. The characteristics of pipe bottom flow get weakened, and the thickness of the cuttings layer decreases further along the flow direction. A small amount of drilling cuttings distributes in the upper part of the inner hole of drill pipe, and the cuttings movement speed is higher than that of the bottom cuttings. The stratified flow characteristic is obvious. The stratified flow can be roughly divided into two layers: most of the cuttings move along the bottom of the inner hole to form the cuttings conveying layer, and some cuttings suspension movement forms the mixed conveying layer. Figure 8(e) shows that the amount of cuttings floating in the flow direction increases and the stratified flow characteristics is obvious when the air velocity is 35 m/s.

3.1.2. Cuttings Distribution along Flow Direction. The distribution of drill cuttings along the flow direction can reflect the accumulation of drill cuttings in the inner hole of drill pipe. The drill pipe-bit model is equally divided into 25 segments along the flow direction, and the amount of drill cuttings at different positions along the flow direction is counted at the time of 2 s, respectively. And, the ratio of the amount of cuttings in different positions to the total number of cuttings in the inner hole of drill pipe is defined as the amount proportion of cuttings along the flow direction which is used to characterize the distribution of cuttings along the flow direction, as shown in Figure 9.

Figure 9 shows that the amount proportion of cuttings along the flow direction increases gradually when the air velocity is 15 m/s. It reaches the maximum in the 3~5 m segment, and the maximum proportion increases with the increase of the mass flow rate of drill cuttings. When the air velocity is 20 m/s, 25 m/s, 30 m/s, and 35 m/s, respectively,

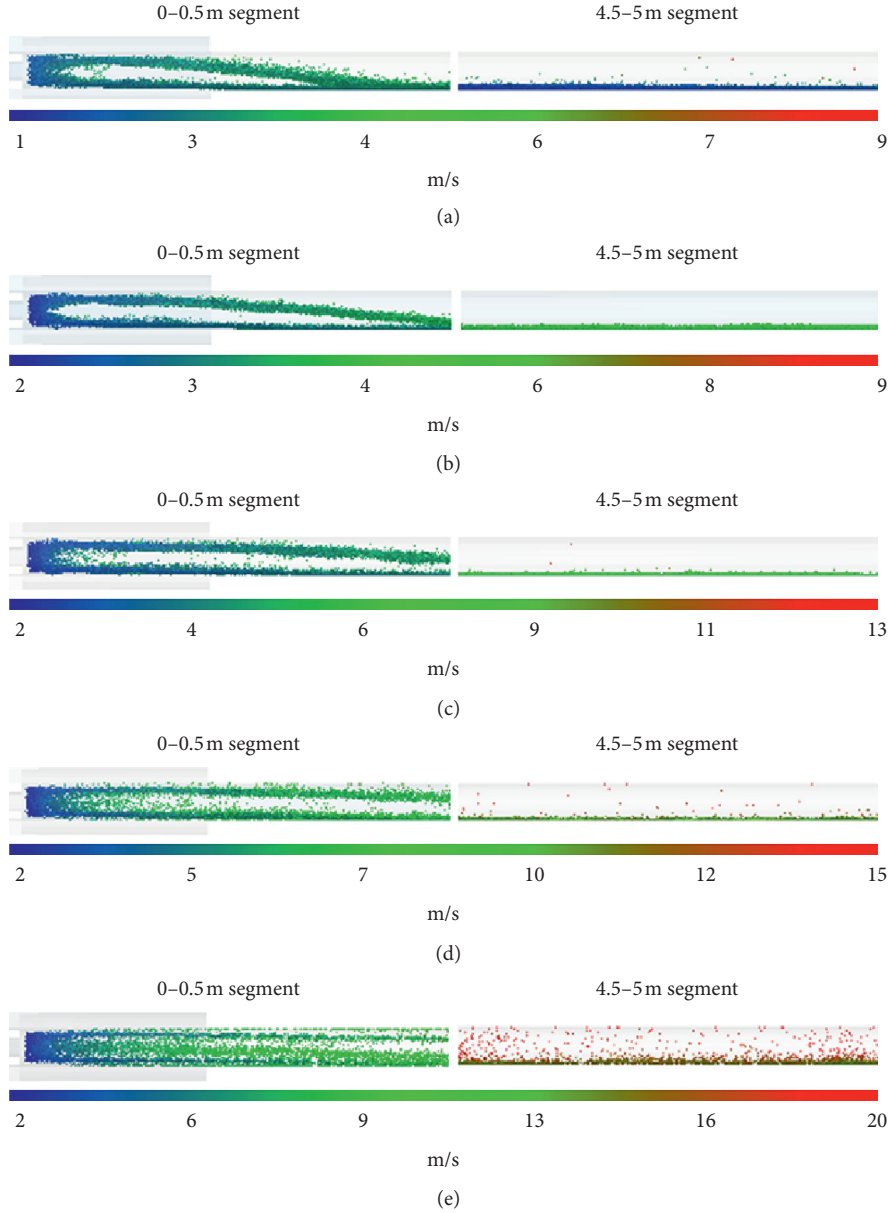


FIGURE 8: Cuttings flow pattern under different gas velocities: (a) $v_a = 15$ m/s, $M_c = 0.14$ kg/s, (b) $v_a = 20$ m/s, $M_c = 0.14$ kg/s, (c) $v_a = 25$ m/s, $M_c = 0.14$ kg/s, (d) $v_a = 30$ m/s, $M_c = 0.14$ kg/s, and (e) $v_a = 35$ m/s, $M_c = 0.14$ kg/s.

the amount proportion of cuttings along the flow direction shows the same trend of change, which gradually decreases along the flow direction and the maximum proportion occurs at the drill bit. The above phenomenon shows that when the air velocity is 15 m/s, the cuttings accumulate in the inner hole of drill pipe. The amount proportion of cuttings along the flow direction increases gradually. With the increase of the mass flow rate of cuttings, the accumulation of drill cuttings intensifies. When the air velocity is 20 m/s, 25 m/s, 30 m/s, and 35 m/s, the cuttings enter the drill bit at a lower initial speed and accelerate under the drag force of the air flow. The cuttings with higher speed are discharged from the inner hole of drill pipe in time, while the cuttings speed at the entrance of the discharge hole of drill bit is relatively low. The amount of cuttings at

the entrance of the discharge hole is higher than that at other positions. Therefore, the amount proportion of cuttings along the flow direction decreases gradually and the maximum proportion increases with the increase of the air velocity.

3.1.3. Cuttings Velocity Variation along Flow Direction.

The variation of drill cuttings velocity along the flow direction can reflect the acceleration and motion characteristics of drill cuttings along the flow direction. The average velocity of drill cuttings at different positions along the flow direction is calculated at time of 2 s separately. The variation of drill cuttings velocity along the flow direction is shown in Figure 10.

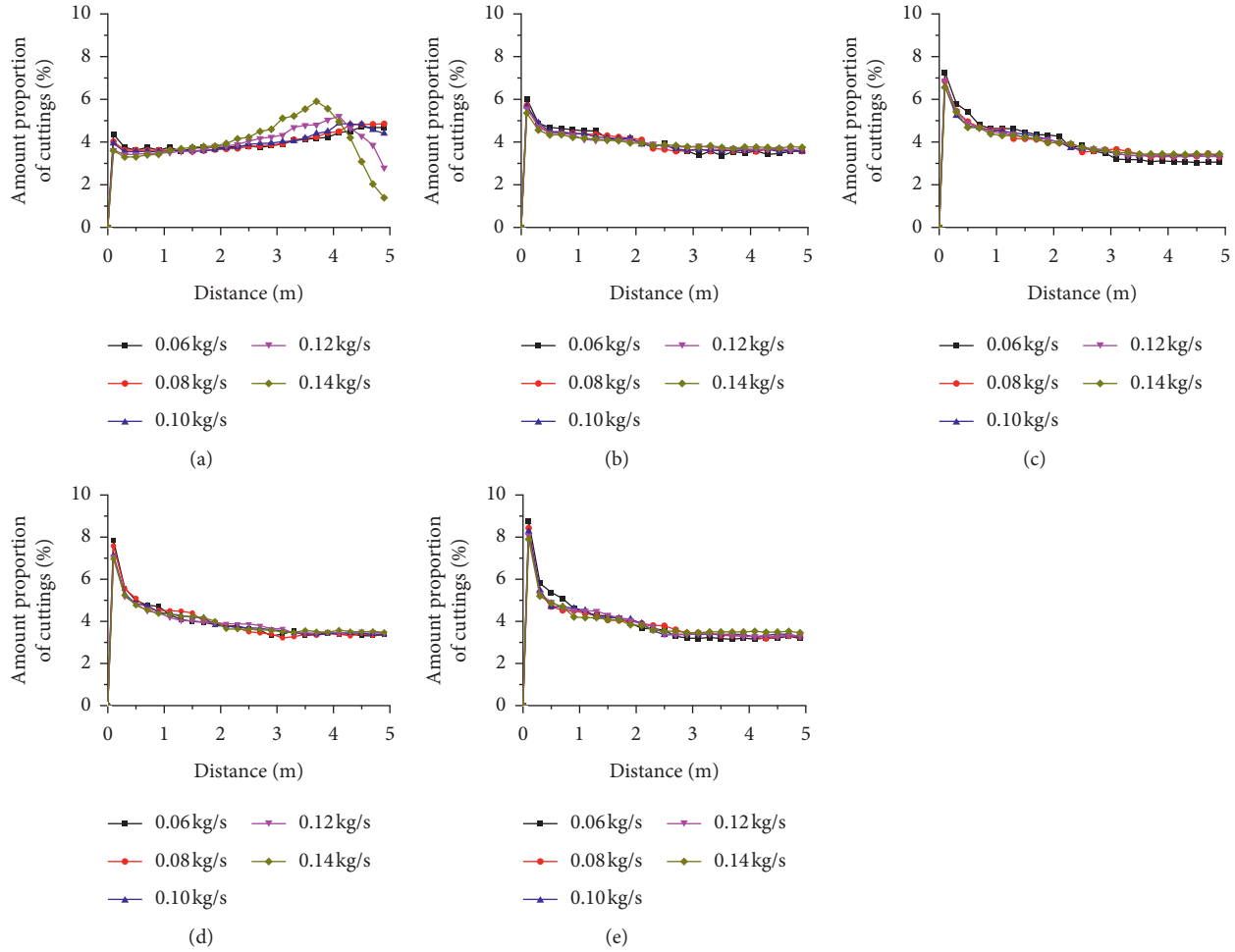


FIGURE 9: Amount distribution of cuttings along flow direction: (a) $v_a = 15$ m/s, (b) $v_a = 20$ m/s, (c) $v_a = 25$ m/s, (d) $v_a = 30$ m/s, and (e) $v_a = 35$ m/s.

As can be seen from Figure 10, when the air velocity is 15 m/s, the drill cuttings enter the inner hole of drill pipe at the initial speed of 2 m/s and accelerate under the drag force of air flow. Drill cuttings decelerate along the flow direction after short-distance acceleration movement. With the increase of the mass flow rate of drill cuttings, the acceleration distance of drill cuttings becomes shorter, the maximum velocity decreases, and the deceleration phenomenon is obvious. When the mass flow rate of cuttings is 0.12 kg/s and 0.14 kg/s, the cuttings decelerate along the flow direction first and accelerate at the end of the drill pipe. As the mass flow rate of drill cuttings increases, the accumulated cuttings increase, the cuttings layer becomes thicker, the area of air flow passage decreases and the air flow velocity increases at this position, which makes the cuttings located at the upper part of the cuttings layer accelerate again. When the air velocity are 20 m/s, 25 m/s, 30 m/s, and 35 m/s, respectively, the cuttings velocity increases along the flow direction. Under the same air velocity, the cuttings velocity at the same position decreases with the increase of the mass flow rate of cuttings. The drag force on the cuttings is proportional to the velocity difference between the cuttings and air flow. When

the cuttings enter the inner hole of drill pipe at a lower initial velocity, the drag force on the cuttings is larger because of the large velocity difference between the cuttings and the air flow. Therefore, the cuttings move in the inner hole of drill pipe with a higher acceleration. With the increase of cuttings velocity, the velocity difference between cuttings and air flow decreases, the drag force decreases, and the acceleration of the cuttings decreases. So, the velocity curve of drill cuttings in the 1~5 m segment is relatively flat compared with that in the 0~1 m segment.

Figures 9 and 10 show the distribution and velocity of the drill cuttings at different positions along the flow direction under different working conditions. In summary, when the air velocity is 15 m/s, the velocity of drill cuttings along the flow direction decreases and accumulates. The cuttings cannot effectively discharge from the inner hole of drill pipe in time and even block the inner hole of drill pipe, which makes the cuttings removal difficult and affects the drilling depth and drilling rate of borehole. When the air velocity is greater than 20 m/s, the velocity of drill cuttings increases along the flow direction, and no accumulation phenomenon occurs, so the cuttings removal can be achieved smoothly.

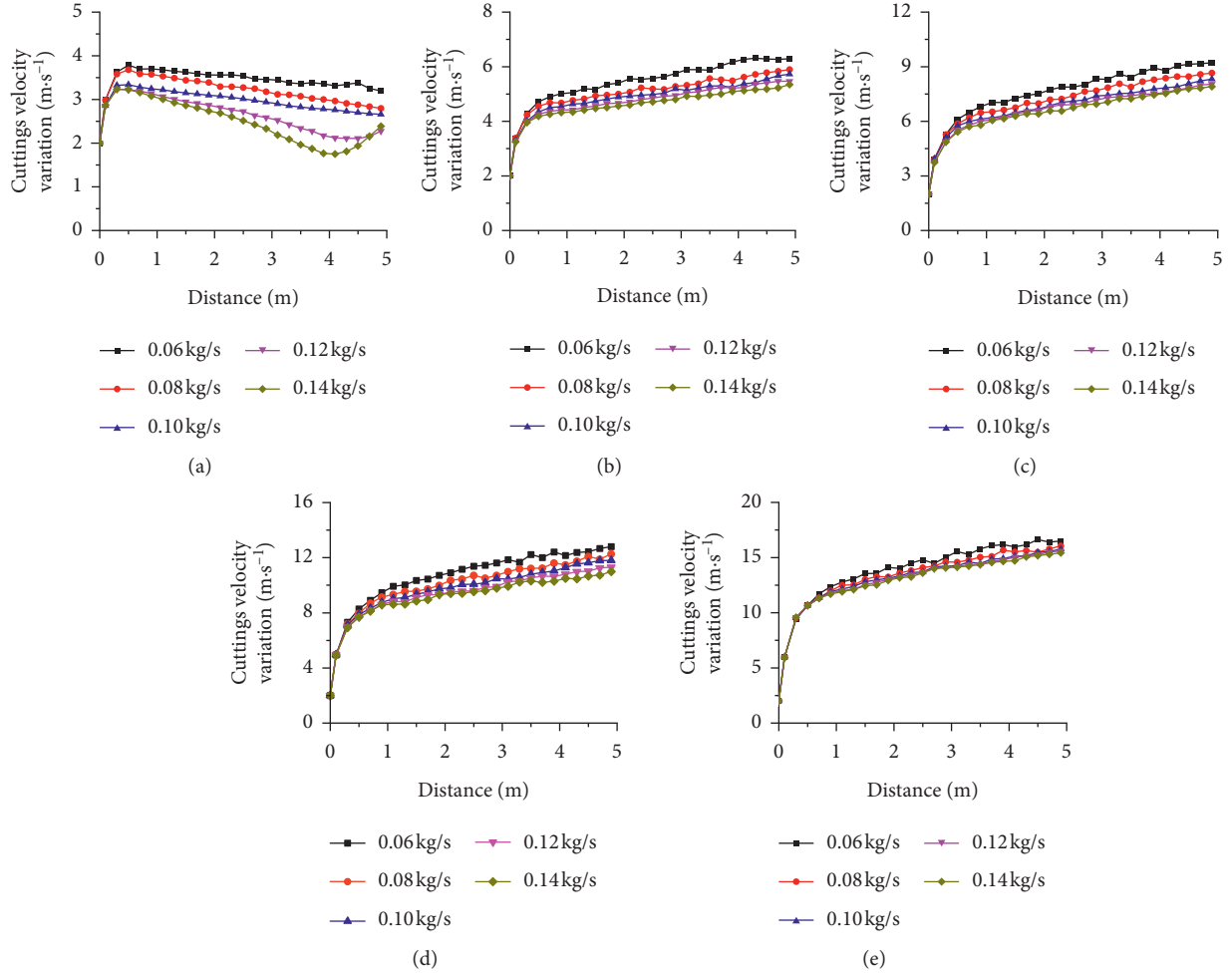


FIGURE 10: Cuttings velocity variation along flow direction: (a) $v_a = 15 \text{ m/s}$, (b) $v_a = 20 \text{ m/s}$, (c) $v_a = 25 \text{ m/s}$, (d) $v_a = 30 \text{ m/s}$, and (e) $v_a = 35 \text{ m/s}$.

When the air velocity is constant, the cuttings mass flow rate increases from 0.06 kg/s to 0.14 kg/s, the amount of drill cuttings increases, and the individual cuttings energy obtained from the air flow decreases. Therefore, the cuttings velocity decreases along the flow direction with the increase of the mass flow rate of cuttings. Similarly, when the mass flow rate of drill cuttings is constant, the individual cuttings energy obtained from the air flow increases with the increase of air velocity. The drill cuttings accelerate faster and move in the inner hole of drill pipe at a higher speed. Therefore, in the application of the new technology of reverse circulation pneumatic cuttings removal, whether the drill cuttings can be discharged from the drilling hole directly depends on the air velocity and the mass flow rate of drill cuttings. In order to ensure that the cuttings are smoothly discharged from the drilling hole, the air velocity cannot be lower than 20 m/s.

3.2. Flow Characteristics Analysis of Air Phase. In order to analyze the influence of operating parameters on the air flow characteristics, the axial air flow velocity distribution at the position of 4.75 m under different cuttings mass flow rate and different air velocity is compared and analysed, as shown in Figure 11.

Figure 11(a) shows the axial airflow velocity distribution at the position of 4.75 m under different mass flow rate of drill cuttings with the air velocity of 30 m/s. It can be seen from the figure that the maximum air flow velocity is distributed in the upper part of the inner hole of drill pipe due to the influence of drill cuttings. With the increase of the mass flow rate of cuttings, the air flow velocity in the lower part decreases while the air flow velocity in the upper part increases, and the position of the maximum air flow velocity moves upward. At the same air velocity, the increase of the mass flow rate of cuttings leads to the increase of the thickness of the bottom cuttings layer, which further reduces the area of air flow passage and aggravates the influence of drill cuttings on the air flow field. The air flow moves upward, and the position of the maximum air flow velocity moves upward.

Figure 11(b) shows the axial flow velocity distribution at the position of 4.75 m under different air velocities with the mass flow rate of 0.14 kg/s. It can be seen from the figure that the position with the maximum air velocity moves downward and gradually approaches the central axis with the increase of the air velocity. When

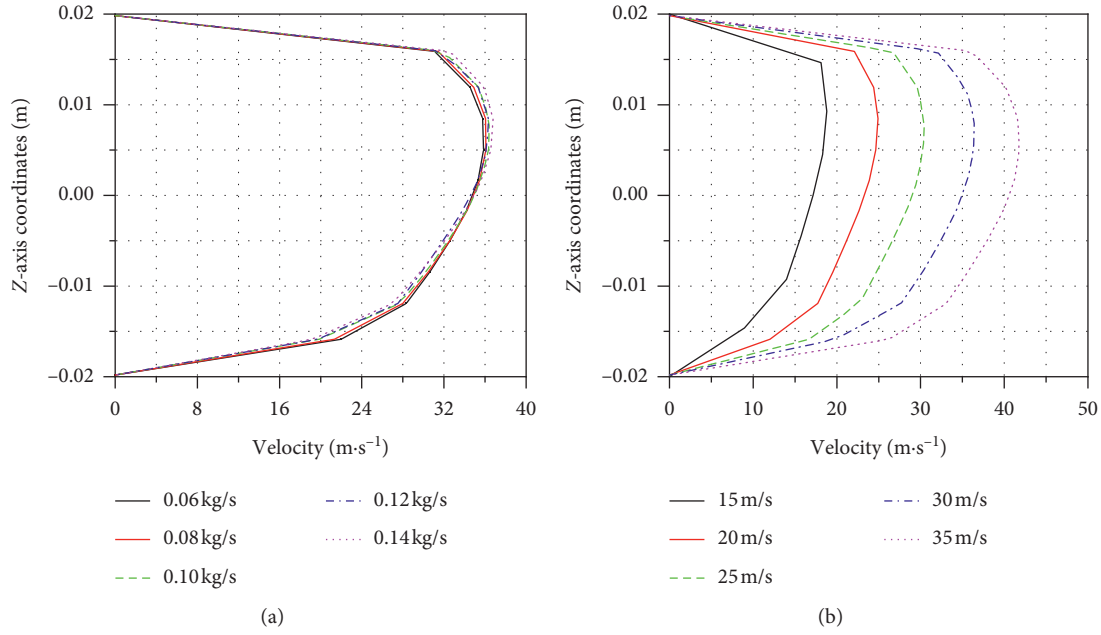


FIGURE 11: Air velocity distribution at position of 4.75 m.

the mass flow rate of cuttings is constant, the cuttings velocity becomes faster with the increase of the air velocity. The cuttings are timely and effectively discharged from the inner hole of drill pipe. So, the corresponding thickness of the bottom drill cuttings layer decreases. Under the higher air velocity, some cuttings move in suspension in the inner hole of drill pipe, which enlarges the air flow passage to weaken the influence of the drill cuttings layer at the bottom of pipe on the airflow. So, the position with the maximum air flow velocity moves downward.

3.3. Forces between Cuttings and Air under Different Working Conditions. In the process of reverse circulation pneumatic cuttings removal, there is a relationship between the action force and the reaction force besides the momentum exchange between drill cuttings and air. The interaction forces between drill cuttings and air in 0~2 s under different working conditions are extracted. As shown in Figure 12, the variation of interaction forces between drill cuttings and air under different working conditions with time is analysed.

Figure 12(a) shows that the interaction forces between drill cuttings and air increase continuously with time when the air velocity is 15 m/s. When the mass flow rate of cuttings is 0.06 kg/s, the interaction forces between two phases increase slowly with time. With the increase of the mass flow rate of cuttings, the slope of the force curves between two phases increase and the forces between two phases increase. When the air velocity is 20 m/s, 25 m/s, 30 m/s, and 35 m/s, respectively, the interaction forces between the cuttings and air increase first. And then, the forces stabilize with time. The time-varying curves of the interaction forces between two phases are divided into the

“growth section” and the “stable section” for analysis. It can be seen that, under the same air velocity, with the increase of the mass flow rate of cuttings, the slope of the “growth section” increases, the corresponding time length increases, and the interaction forces between the two phases of the “stable section” increase. When the mass flow rate of cuttings is constant, the slope of the “growth section” curve increases with the increases of the air velocity, and the corresponding time length becomes shorter, while the interaction forces between the two phases in the “stable section” become larger. When the air velocity is greater than 20 m/s, there is no accumulation of drill cuttings in the inner hole of drill pipe. The amount of drill cuttings in the drill pipe reaches the dynamic balance state and the interaction forces between the two phases remain relatively stable. When the mass flow rate of cuttings keeps constant, with the increase of the air velocity, the movement speed of drill cuttings becomes faster, and the time of reaching the “stable section” of the interaction forces between two phases becomes shorter. Although the increase of air velocity decreases the number of cuttings in the drill pipe, the drag force of a single cuttings by the flow field increases significantly at this time. So, the interaction forces between the two phases tend to increase. At the same air velocity, with the increase of the mass flow rate of cuttings, the amount of cuttings in the drill pipe increases and the interaction forces between the two phases increase. At the same time, the increase of the number of drill cuttings slows down the cuttings velocity. So, the time when the interaction forces between two phases reach the “stable section” becomes longer. It can be seen that the variation of the interaction forces between drill cuttings and air with time can be used to judge whether the cuttings-air two-phase flow reaches a stable state in the simulation process.

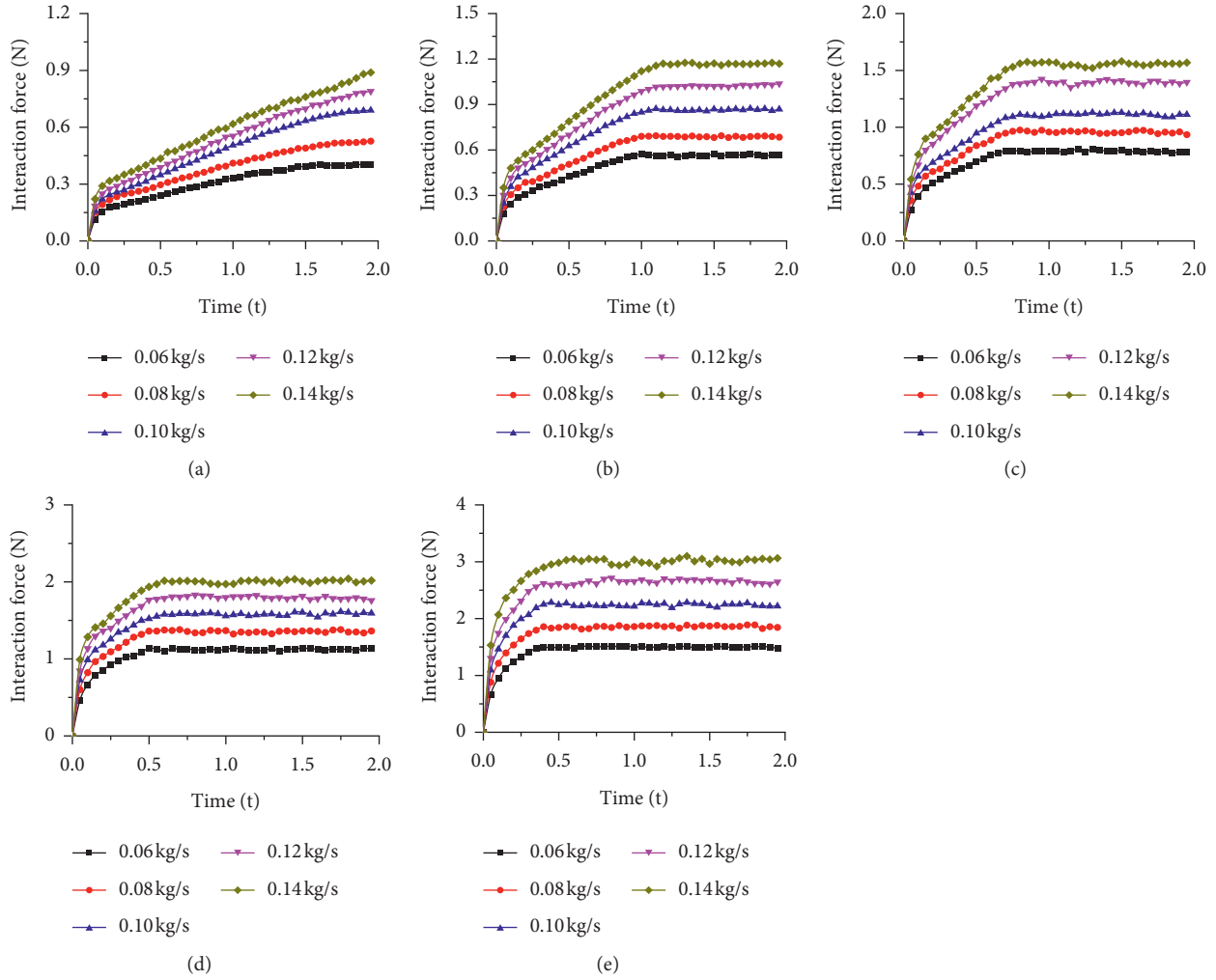


FIGURE 12: Interaction forces between cuttings and air: (a) $v_a = 15$ m/s, (b) $v_a = 20$ m/s, (c) $v_a = 25$ m/s, (d) $v_a = 30$ m/s, and (e) $v_a = 35$ m/s.

3.4. Cuttings Removal Effect under Different Working Conditions. In order to analyze the influence of different working conditions on the effect of reverse circulation pneumatic cuttings removal, the cuttings migration ratio is used to evaluate the cuttings removal effect [22]. The cuttings migration ratio is defined as the ratio of the average cuttings velocity in the drill pipe to the air velocity under the corresponding working conditions. Figure 13 shows the cuttings migration ratio under different working conditions.

Figure 13 shows that, when the mass flow rate of cuttings is constant, the cuttings migration ratio is positively correlated with the air velocity, while when the air velocity is constant, the cuttings migration ratio is negatively correlated with the mass flow rate of cuttings. In addition, when the air velocity is low, the difference between the cuttings migration ratios under different mass flow rate of cuttings is large. With the increase of the air velocity, the difference between the cuttings migration

ratios under different mass flow rate of cuttings decreases gradually. Drill cuttings move along the flow direction with the characteristics of pipe bottom flow under the action of airflow drag force and self-gravity after entering the inner hole of drill pipe. When the air velocity is low, the pipe bottom flow characteristics are significant. At this time, the collision and friction between cuttings-cuttings, drill pipe-cuttings have a greater influence on the cuttings movement, which result in the average velocity of drill cuttings far lower than the air velocity. The effect of cuttings removal is poor. With the increase of air velocity, the characteristics of pipe bottom flow weaken, and some drill cuttings move in suspension in the inner hole of drill pipe. The collision and friction between cuttings-cuttings, drill pipe-cuttings decrease. So, the cuttings migration ratio increases. When the air velocity is constant, the increase of the mass flow rate of cuttings increases the amount of cuttings in the drill pipe. The influence of collision and friction between cuttings-

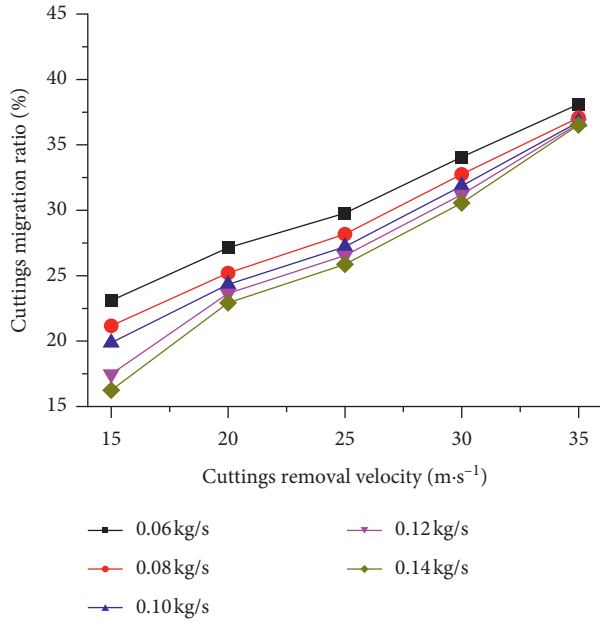


FIGURE 13: Cuttings migration ratio under different working conditions.

cuttings, drill pipe-cuttings on the cuttings movement is intensified. So, the cuttings removal effect becomes worse. Compared with the low air velocity, the higher air velocity can make the drill cuttings be discharged from the drill pipe in time and effectively. The amount of drill cuttings in the drill pipe is relatively small. The increase of the mass flow rate of cuttings has little effect on the cuttings movement. Therefore, under the condition of low air velocity, the cuttings migration ratio varies greatly with different mass flow rate of cuttings. Under the condition of high air velocity, the increase of mass flow rate of cuttings has little effect on the cuttings migration ratio.

3.5. Pressure Drop of Cuttings-Air Two-Phase Flow. The drill cuttings generated by the drilling bit breaking coal enter the inner hole of drill pipe under the action of air flow and discharge along the flow direction. In this process, all kinds of energy consumed by air flow and drill cuttings movement are compensated by the pressure energy of the air flow. So, the pressure drop of air flow can be used to characterize the energy consumption of cuttings-air two-phase flow [23]. The pressure drop of cuttings-air two-phase flow in the inner hole of drill pipe under different working conditions is shown in Figure 14.

As can be seen from Figure 14, the pressure drop of cuttings-air two-phase flow is significantly higher than that in the inner hole of drill pipe under the pure air flow, which indicates that the drill cuttings cause the greater energy consumption to the air flow. The pressure drop shows the same trend with the increase of air velocity under different mass flow rate of cuttings. At the same mass flow rate of cuttings, the pressure drop increases with the increase of air velocity. And, at the same air velocity, the pressure drop also increases with the increase of the mass flow rate of cuttings.

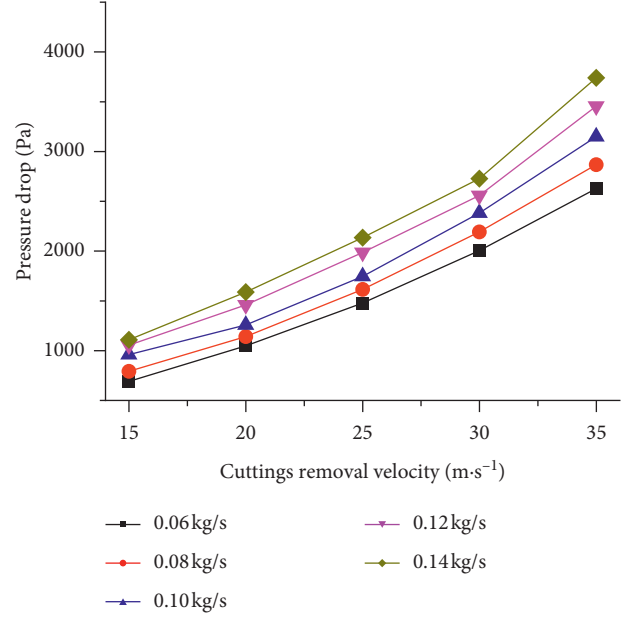


FIGURE 14: Air flow pressure drop under different working conditions.

The pressure drop in the inner hole of drill pipe is mainly composed of two parts. One part is the friction pressure drop of air flow. The other part is the pressure drop caused by the drill cuttings which includes the energy consumption caused by the collision and friction among cuttings-cuttings and drill pipe-cuttings during the cuttings removal and the kinetic energy obtained by the drill cuttings. When the mass flow rate of cuttings is constant, the mixing ratio of drill cuttings to air decreases with the increase of the air velocity, but the friction pressure drop of air flow and the kinetic energy of drill cuttings increases. So, the pressure drop increases with the increase of the air velocity. At the same air velocity, with the increase of the mass flow rate of cuttings, the mixing ratio of cuttings and air increases and the porosity in the inner hole of drill pipe decreases. At this time, the energy consumption increases due to the collision and friction among cuttings-cuttings and cuttings-drill pipe, so the pressure drop also increases with the increase of the mass flow rate of cuttings.

In conclusion, the higher air velocity increases the pressure drop of air flow and the air consumption. Therefore, in order to avoid unnecessary energy consumption, on the premise of ensuring the smooth discharge of drill cuttings from the drill hole, the appropriate air velocity should be selected to determine the air volume of Roots vacuum pump. Taking the simulation model in this paper as an example, when the air velocity is 15 m/s, the amount of cuttings increases along the flow direction, and the velocity of cuttings decreases. So, the drill cuttings will accumulate in the inner hole of drill pipe. If the air velocity is greater than 20 m/s, the amount of cuttings will decrease along the flow direction. The speed and pressure drop of drill cuttings will increase. So, 20 m/s is selected as the appropriate air velocity of cuttings removal.

4. Conclusions

In this paper, the CFD-DEM coupling method is used to simulate the two-phase flow of drill cuttings and air in the inner hole of drill pipe with the reverse circulation pneumatic cuttings removal technology during the horizontal drilling in coal seam. The effects of the air velocity and the mass flow rate of cuttings on the two-phase flow characteristics, cuttings removal effect, and pressure drop of the flow field are analysed. The results show that the following:

- (1) With the increase of air velocity, the drag force of drilling cuttings becomes larger. The characteristic length of drilling cuttings flow becomes longer. The thickness of the cuttings layer decreases further along the flow direction. A small amount of drilling cuttings distributes in the upper part of the inner hole of drill pipe and the cuttings movement speed is higher than that of the bottom cuttings. The stratified flow characteristic is obvious.
- (2) When the air velocity of cuttings removal is 15 m/s, the proportion of drill cuttings along the flow direction increases, the forces between the cuttings and air increase continuously with time, and the cuttings velocity decreases. So, the drill cuttings are easy to accumulate in the inner hole of drill pipe. If the air velocity is greater than 20 m/s, the proportion of cuttings along the flow direction decreases and the cuttings velocity increases.
- (3) When the mass flow rate of cuttings is constant, the cuttings migration ratio is positively correlated with the air velocity. When the air velocity is constant, the cuttings migration ratio is negatively correlated with the mass flow rate of cuttings. The interaction forces between drill cuttings and air increase first. And then, the forces stabilize with time.
- (4) At the same mass flow rate of cuttings, the pressure drop of the cuttings-air two-phase flow increases with the increase of air velocity. At the same air velocity, the pressure drop of the cuttings-air two-phase flow increases with the increase of the mass flow rate of cuttings. So, 20 m/s is selected as the appropriate air velocity for cuttings removal considering the pressure drop of cuttings-air two-phase flow and the flow characteristics of drill cuttings.

Data Availability

The data used to support the findings of this study are available from the corresponding author upon request.

Conflicts of Interest

The authors declare that there are no conflicts of interest regarding the publication of this paper.

Acknowledgments

This work was supported by the Natural Science Foundation of Henan Province (grant no. 182300410156), the Open Foundation of Henan Coal Mine Machinery Equipment Engineering Technology Research Center (grant no. MKJXZB202006), and the Innovation Team Project of Nonlinear Equipment Dynamics (grant no. T2019-5).

References

- [1] C. Liu, *Study on mechanism and controlling of borehole collapse in soft coal seam*, Ph.D. thesis, China University of Mining and Technology, Xuzhou, China, 2014.
- [2] N. Yao, X. Yin, Y. Wang, L. Wang, and Q. Ji, "Practice and drilling technology of gas extraction borehole in soft coal seam," *Procedia Earth and Planetary Science*, vol. 3, pp. 53–61, 2011.
- [3] Y.-L. Wang, Y.-N. Sun, X.-X. Zhai, and Z.-F. Wang, "Study on new drilling technology in soft and outburst seam," *Journal of Mining and Safety Engineering*, vol. 29, no. 2, pp. 289–294, 2012.
- [4] Y. L. Wang, Z. F. Wang, and W. Y. Lu, "Analysis on pressure loss of drill cuttings movement caused by gas-solid coupling in gas extraction borehole," *Science and Technology of Safety Production in China*, vol. 4, pp. 13–19, 2015.
- [5] X.-M. Han, L.-L. Zhang, Y. Liu, and Z.-H. Tie, "Chip removal mechanism by air reverse circulation during horizontal drilling in soft outburst coal seam," *Science and Technology of Safety Production in China*, vol. 11, no. 5, pp. 26–31, 2015.
- [6] X. M. Han, S. N. Song, and J. L. Li, "Pressure drop characteristics of reverse circulation pneumatic cuttings removal during coal seam drilling," *Science Progress*, vol. 103, no. 2, pp. 1–20, 2020.
- [7] G. Niu and W. Zhang, "Study on critical air velocity and pressure loss of pneumatic coal dust removal for boreholes along coal seams," *China Safety Science Journal*, vol. 23, no. 11, pp. 60–65, 2013.
- [8] B. Guo, T. A. G. Langrish, and D. F. Fletcher, "CFD simulation of precession in sudden pipe expansion flows with low inlet swirl," *Applied Mathematical Modelling*, vol. 26, no. 1, pp. 1–15, 2002.
- [9] A. Riaz and M. A. Sadiq, "Particle-fluid suspension of a non-newtonian fluid through a curved passage: an application of urinary tract infections," *Frontiers in Physics*, vol. 8, p. 109, 2020.
- [10] A. Riaz, A. Zeeshan, S. Ahmad, A. Razaq, and M. Zubair, "Effects of external magnetic field on non-Newtonian two phase fluid in an annulus with peristaltic pumping," *Journal of Magnetism*, vol. 24, no. 1, pp. 62–69, 2019.
- [11] S. I. Abdelsalam, M. M. Bhatti, A. Zeeshan, A. Riaz, and O. A. Bég, "Metachronal propulsion of a magnetised particle-fluid suspension in a ciliated channel with heat and mass transfer," *Physica Scripta*, vol. 94, no. 11, Article ID 115301, 2019.
- [12] N. Ijaz, A. Riaz, A. Zeeshan, R. Ellahi, and S. M. Sait, "Buoyancy driven flow with gas-liquid coatings of peristaltic bubbly flow in elastic walls," *Coatings*, vol. 10, no. 2, p. 115, 2020.
- [13] J.-W. Zhou, C.-L. Du, S.-Y. Liu, and Y. Liu, "Comparison of three types of swirling generators in coarse particle pneumatic conveying using CFD-DEM simulation," *Powder Technology*, vol. 301, pp. 1309–1320, 2016.

- [14] J.-W. Zhou, Y. Liu, S.-Y. Liu, C.-L. Du, and J.-P. Li, "Effects of particle shape and swirling intensity on elbow erosion in dilute-phase pneumatic conveying," *Wear*, vol. 380-381, pp. 66-77, 2017.
- [15] P. W. Jian, H. T. Zhang, and Y. G. Wang, "The gas-solid flow characteristics of cyclones," *Powder Technology*, vol. 308, pp. 178-129, 2017.
- [16] S. Akhshik, M. Behzad, and M. Rajabi, "CFD-DEM approach to investigate the effect of drill pipe rotation on cuttings transport behavior," *Journal of Petroleum Science and Engineering*, vol. 127, pp. 229-244, 2015.
- [17] S. Akhshik, M. Behzad, and M. Rajabi, "CFD-DEM simulation of the hole cleaning process in a deviated well drilling: the effects of particle shape," *Particuology*, vol. 25, pp. 72-82, 2015.
- [18] B. Shao, Y. F. Yan, and C. F. Bi, "Migration of irregular cuttings particles in big size by CFD-DEM coupled simulation model," *Science, Technology and Engineering*, vol. 17, no. 27, pp. 195-200, 2017.
- [19] B. Sun, H. Xiang, H. Li, and X. Li, "Modeling of the critical deposition velocity of cuttings in an inclined-slimhole annulus," *SPE Journal*, vol. 22, no. 4, pp. 1213-1224, 2017.
- [20] Y.-J. Kim, N.-S. Woo, Y.-K. Hwang, J.-H. Kim, and S.-M. Han, "Transport of small cuttings in solid-liquid flow with inclined slim hole annulus," *Journal of Mechanical Science and Technology*, vol. 28, no. 1, pp. 115-126, 2014.
- [21] Z. L. Yuan, L. P. Zhu, and F. Geng, *Gas-Solid Two Phase Flow and Numerical Simulation*, Southeast University Press, Nanjing, China, 2013.
- [22] M. Sorgun, "Simple correlations and analysis of cuttings transport with Newtonian and non-Newtonian fluids in horizontal and deviated wells," *Journal of Energy Resources Technology*, vol. 135, no. 3, Article ID 032903, 6 pages, 2013.
- [23] C. Liang, L. Shen, P. Xu et al., "Comparison of pressure drops through different bends in dense-phase pneumatic conveying system at high pressure," *Experimental Thermal and Fluid Science*, vol. 57, pp. 11-19, 2014.